Xudong Zhu, Guijuan Zong, Liu Zhu, Yuchen Jiang, Ke Ma, Hanwen Zhang, Yan Zhang, Hui Bai, Qing Yang, Jingjing Ben, Xiaoyu Li, Yong Xu, Qi Chen

OBESITY STUDIES

Deletion of Class A Scavenger Receptor Deteriorates Obesity-Induced Insulin Resistance in Adipose Tissue

Chronic low-grade inflammation, particularly in the adipose tissue, orchestrates obesity-induced insulin resistance. In this process, polarized activation of macrophages plays a crucial role. However, how macrophages contribute to insulin resistance remains obscure. Class A scavenger receptor (SR-A) is a pattern recognition receptor primarily expressed in macrophages. Through a combination of in vivo and in vitro studies, we report here that deletion of SR-A resulted in reduced insulin sensitivity in obese mice. The anti-inflammatory virtue of SR-A was accomplished by favoring M2 macrophage polarization in adipose tissue. Moreover, we demonstrate that lysophosphatidylcholine (LPC) served as an obesity-related endogenous ligand for SR-A promoting M2 macrophage polarization by activation of signal transducer and activator of transcription 6 signaling. These data have unraveled a clear mechanistic link between insulin resistance and inflammation mediated by the LPC/SR-A pathway in macrophages.

Obesity is the most important risk factor associated with insulin resistance and type 2 diabetes. The mechanisms linking obesity to insulin resistance have been investigated extensively. Over the past decade, numerous studies have revealed that inflammatory signaling pathways in obesity are causally linked to insulin resistance (1,2). Accumulation of macrophages in the adipose tissue has been suggested as a function of body weight and correlates with measures of insulin resistance. These adipose tissue macrophages (ATMs) stimulate adipose tissue inflammation by secreting proinflammatory adipokines, leading to systemic insulin resistance (3–6).

ATMs consist of at least two different subpopulations (i.e., classically activated M1 macrophages and alternatively activated M2 macrophages) based on their anatomical location and functional phenotype. M1/M2 ATMs have distinct functions in the regulation of insulin sensitivity. For example, M2 macrophages can maintain the insulin sensitivity of adipocytes. In contrast, M1 macrophages secrete proinflammatory cytokines to induce insulin resistance (7,8). Thus, inhibiting inflammatory signals within ATMs could serve as a therapeutic strategy for obesity-related metabolic disorders. Despite recent advances in the understanding of ATM-modulated insulin signaling, the upstream mechanisms for detecting, initiating, and activating the proinflammatory pathways in ATMs remain to be fully elucidated.

Class A scavenger receptor (SR-A) is a pattern recognition receptor (PRR) mainly expressed on the surface of

---

Corresponding author: Qi Chen, qichen@njmu.edu.cn.

macrophages. It is a multifunctional molecule characterized by its ability to recognize and bind with a broad spectrum of ligands and by its flexible modulation in internalization (9–12). Rasouli et al. (13) have reported that there is a strong association of upregulation of SR-A in the adipose tissue with insulin resistance in non-diabetic humans. We investigated the impact of SR-A on obesity-induced insulin resistance in both genetically obese (*ob/ob*) mice and mice with diet-induced obesity (DIO). We found that SR-A deficiency reduced insulin sensitivity in these mice, which could be attributed to a diminished M2 macrophage population and increased inflammatory response in the adipose tissue. We also demonstrated that lysophosphatidylcholine (LPC) could function as an obesity-sensitive endogenous ligand for SR-A to promote M2 macrophage polarization through activation of signal transducer and activator of transcription (STAT)6. Taken together, the results of the current study establish a molecular link between LPC/SR-A and obesity-induced insulin resistance.

RESEARCH DESIGN AND METHODS

Animals

SR-A$^{-/-}$ breeding pairs, on a C57BL/6 background, were purchased from The Jackson Laboratory. Animals were housed under a 12-h light/dark cycle under pathogen-free conditions with free access to mouse chow and water. All animal care and use was in accordance with guidelines established by the Research Animal Care Committee of Nanjing Medical University. C57BL/6 SR-A$^{+/+}$ and SR-A$^{-/-}$ male mice were fed a high-fat diet (HFD) or a nutrient-matched standard-fat chow diet (58% kcal from fat and 11% kcal from fat, respectively; Research Diets, New Brunswick, NJ) starting at age 6 weeks.

Generation of *ob/ob* Mice Deficient in SR-A

Mice deficient in SR-A (SR-A$^{-/-}$; C57BL/6) were intercrossed with *OB/ob* mice (The Jackson Laboratory) to produce animals heterozygous at the SR-A and *ob* loci (SR-A$^{+/-}$, *OB/ob*), which also involved two additional back-crosses to C57BL/6, the background strain of the *ob/ob* mutation. The resulting double heterozygote animals were cross-bred with each other to produce obese littermates with mutations in SR-A (SRA$^{-/-}$*ob/ob*) and with intact functional SR-A as controls (SRA$^{+/+}$*ob/ob*).

Bone Marrow Transplantation

Murine total bone marrow hematopoietic progenitor donor cells were harvested from SR-A$^{+/+}$*ob/ob* or SR-A$^{-/-}$*ob/ob* C57BL/6 male mice and were transplanted via tail vein injection into lethally irradiated SR-A$^{-/-}$*ob/ob* C57BL/6 male mice (900 rads; Cobalt-60 source) with a minimum cell dose of 5 × 10^6 mononuclear cells per mouse. Transplanted mice were housed in microisolator housing for 6 weeks and for subsequent insulin sensitivity analyses.

Intraperitoneal Glucose and Insulin Tolerance Tests

Mice were injected intraperitoneally with 10% (w/v) glucose (1.0 g/kg) for glucose tolerance test (GTT) or insulin (1.0 units/kg) for insulin tolerance test (ITT), respectively. Glucose levels were monitored via tail vein blood sampling using the OneTouch Horizon Glucose Monitoring kit (LifeScan, Milpitas, CA). Insulin secretory response was monitored in overnight-fasted animals. Insulin levels were measured with a radioimmunoassay kit (Bnibt, Beijing, China).

Stromal Vascular Fraction Isolation and Purification

Epididymal fat pads were minced, and adipocytes and stromal vascular fractions (SVFs) were separated by collagenase (1.5 mg/mL; Sigma-Aldrich, St. Louis, MO) digestion. Stromal vascular cells were filtered, blocked in PBS/2% BSA, and stained with fluorescently labeled antibodies: F4/80-Alexa488, CD11c-Alexa647, or CD301-Alex647 as indicated (AbD Serotec, Oxford, U.K.).

Cell Culture

Peritoneal macrophages (PMs) were harvested as previously described (11). GM-CSF–dependent and M-CSF–dependent bone marrow–derived macrophages were generated as mentioned previously (14). Briefly, bone marrow cells were flushed from long bones of mice in RPMI 1640 medium and centrifuged, and the cell pellet was resuspended (10^6 cells/mL) in RPMI 1640 containing either 20 ng/mL M-CSF (Sigma-Aldrich) or 50 ng/mL GM-CSF (Sigma-Aldrich). After 3 days, nonadherent cells were harvested and 3 × 10^6 cells were seeded in 10 mL of the same medium in nontreated 100-mm dishes for another 4 days.

Macrophage Phagocytosis and Chemotaxis Assay

Macrophage phagocytosis of zymosan was assessed using the CytoSelect 96-well phagocytosis assay kit (Cell Biolabs, San Diego, CA) according to the manufacturer's protocol. Macrophage chemotaxis in response to MCP-1 (R&D Systems) and 10% FBS was performed using the CytoSelect 96-well cell migration assay kit (Cell Biolabs) according to the manufacturer's protocol.

Quantitative RT-PCR

RNA extraction was performed with an RNAiso Plus (TaKaRa, Shiga, Japan). Real-time reactions were performed using standard methods, and real-time PCR analysis was normalized to glyceraldehyde-3-phosphate dehydrogenase (GAPDH) (ABI Prism 7500 Sequence Detection System; Applied Biosystems).

Immunoprecipitation

Five minutes after the insulin injection (3.8 units/kg i.p.), adipose tissues were removed, minced coarsely, and homogenized immediately in extraction buffer. For immunoprecipitations, lysates were incubated with 1 μg anti-insulin receptor (IR)β antibodies (Abcam, Cambridge, MA) overnight at 4°C and immune complexes precipitated
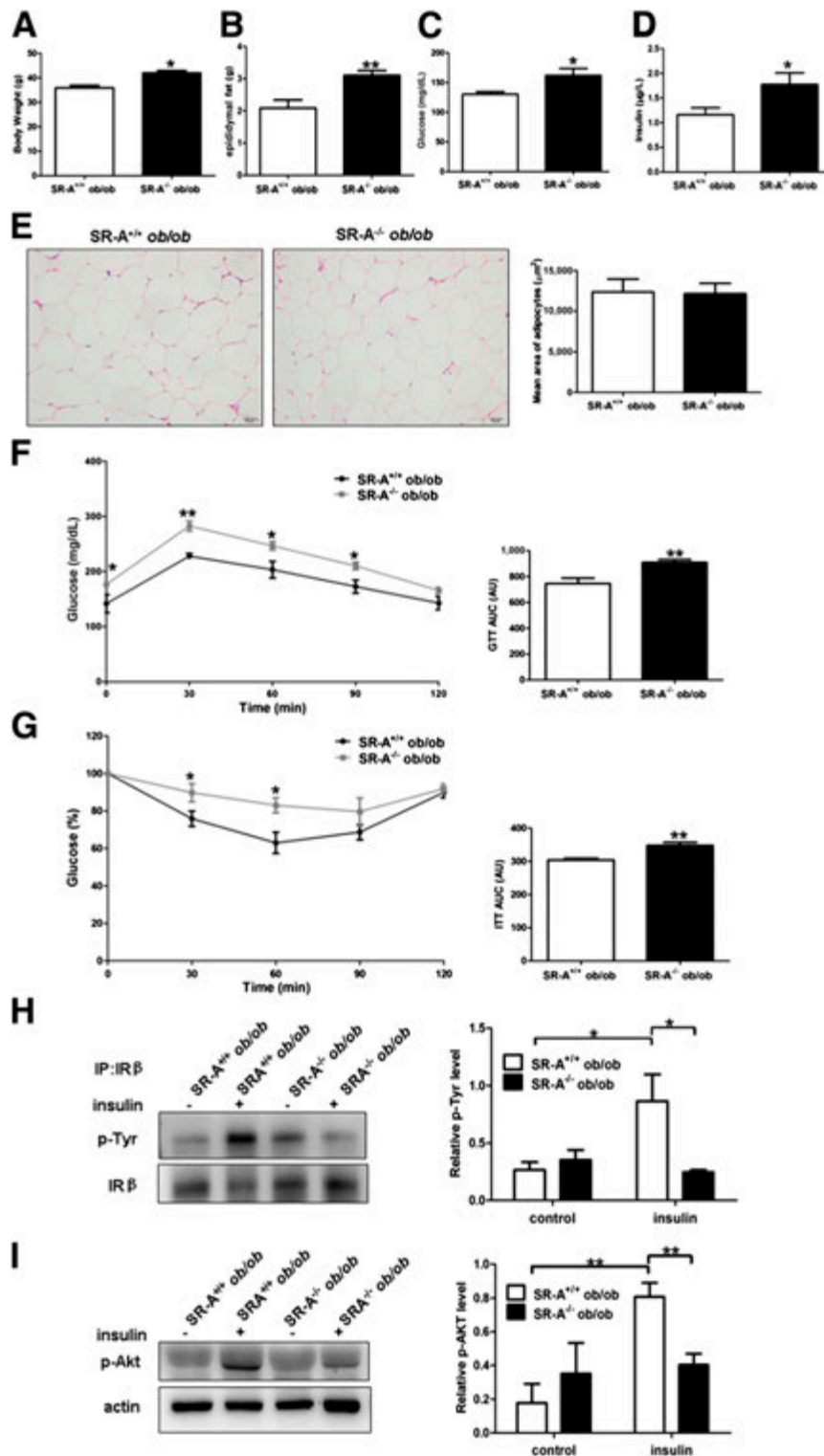
Figure 1—Loss of SR-A in the *ob/ob* background deteriorates insulin sensitivity. *A–E*: SR-A$^{+/+}$*ob/ob* and SR-A$^{-/-}$*ob/ob* mice were an-alyzed when they were 9 weeks old. The body weight (*A*), epididymal fat pad weight (*B*), fasting plasma glucose (*C*), and fasting serum insulin concentrations (*D*) of mice were measured. Histological sections of epididymal fat pads were quantitatively analyzed in adipocyte size by Image-Pro Plus software (*E*). $n = 6$. *F* and *G*: GTT (*F*) and ITT (*G*) were performed. Area under the curve (AUC) of GTT and ITT was calculated and is expressed as arbitrary units (AU). $n = 6$. *H* and *I*: The representative blots of insulin signaling in the adipose tissue of SR-A$^{+/+}$*ob/ob* and SR-A$^{-/-}$*ob/ob* mice administered with insulin. The lysates were immunoprecipitated with IRβ antibody and immunoblotted with phospho-Tyr (p-Tyr) and IRβ antibody. Relative band intensities were normalized to IRβ. $n = 3$ (*H*). The lysates were immunoblotted with phospho-Akt (p-Akt) and β-actin antibody. Relative band intensities were normalized to β-actin. $n = 3$ (*I*). Data are expressed as mean ± SEM. *$P < 0.05$; **$P < 0.01$. IP, immunoprecipitation.
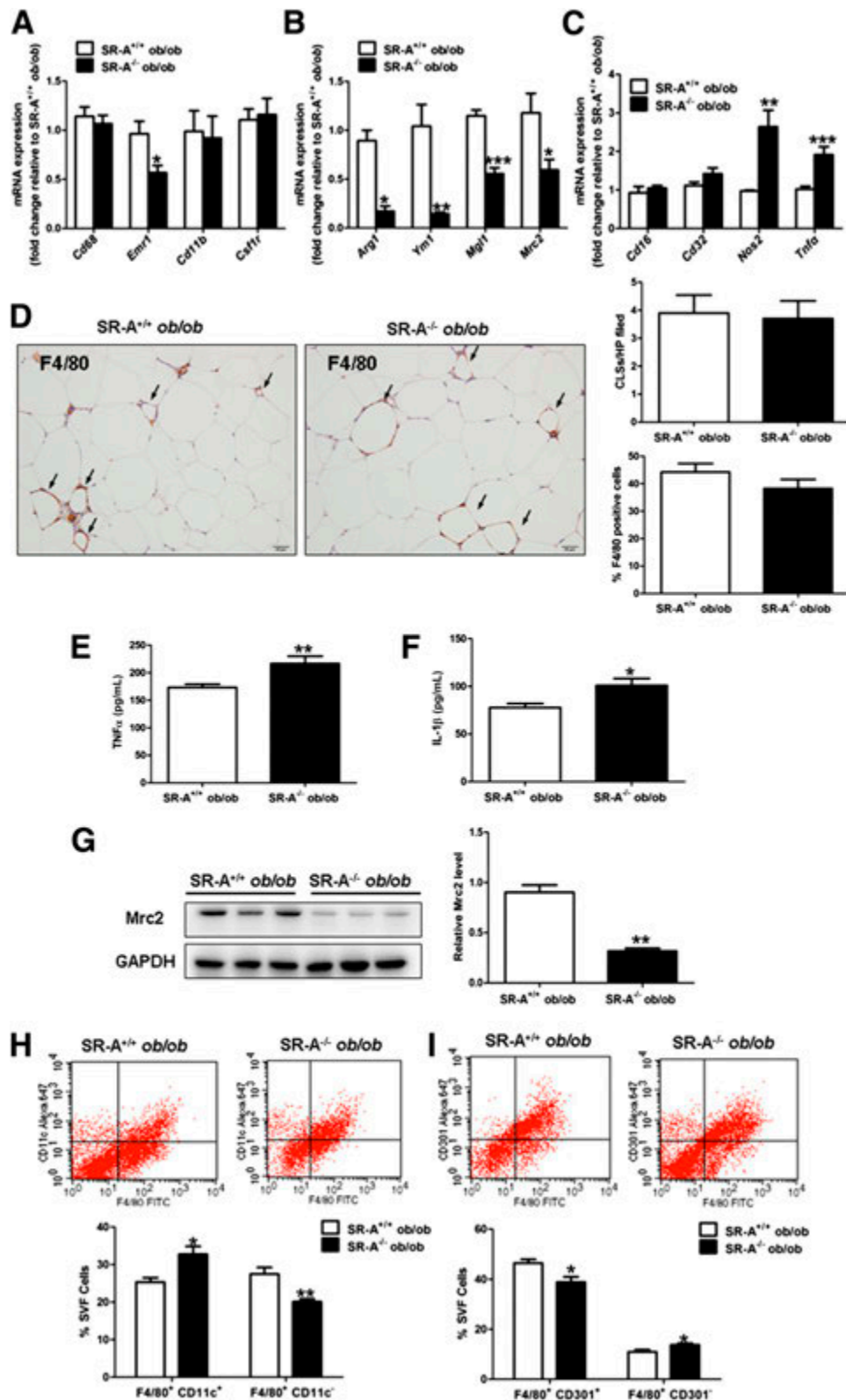
Figure 2—Loss of SR-A promotes a skewed M1/M2 ATM polarization in *ob/ob* mice. *A*: Expression of macrophage/myeloid cell–specific genes was analyzed in the epididymal fat tissue. Expression levels were normalized first to those of GAPDH and then further normalized to those of SR-A^{+/+}*ob/ob* mice. *n* = 5. *B* and *C*: SVF cells were isolated from epididymal fat pads. Levels of mRNA expression of M2 macrophage–associated genes (*B*) and M1 macrophage–associated genes (*C*) were analyzed. Expression levels were normalized first to those of GAPDH and then further normalized to those of SR-A^{+/+}*ob/ob* cells. *n* = 5. *D*: Immunohistochemical staining for F4/80 in epididymal fat pad sections. The number of CLSs (brown staining, see arrows) and F4/80-positive cells relative to total number of cells was determined for both SR-A^{+/+}*ob/ob* and SR-A^{−/−}*ob/ob* mice (6–10 images at ×20 magnification were analyzed per mouse). *n* = 5. *E* and *F*: Plasma levels of TNF-α (*E*) and IL-1β (*F*) were obtained using ELISA assay. *n* = 6. *G*: The blots of Mrc2 in the adipose tissue of SR-A^{+/+}*ob/ob*

with Protein A/G–conjugated beads (Santa Cruz Biotechnology, Santa Cruz, CA).

Histological Analysis

Tissue samples for histology were fixed in 4% paraformaldehyde in PBS overnight, and paraffin-embedded sections were prepared (4-μm sections). Sections of adipose tissues were incubated with anti-F4/80 (AbD Serotec, Oxford, U.K.).

Measurement of LPC

Lipid extracts from adipose tissue were prepared according to Folch et al. (15). LPC concentrations in lipid extracts and in plasma were determined by using an enzyme tic assay (16). Each sample (10 μL) was mixed with 240 μL reaction buffer containing 100 mmol/L Tris-HCl (pH 8.0), 0.01% Triton X-100, 1 mmol/L calcium chloride, 3 mmol/L TOOS, 10 kU/L peroxidase, 0.1 kU/L glycerophosphorylcholine phosphodiesterase, and 10 kU/L choline oxidase. After incubation for 5 min at 37°C, 80 μL lysophospholipase buffer containing 100 mmol/L Tris-HCl (pH 8.0), 0.01% Triton X-100, 5 mmol/L 4-aminoantipyrine, and 30 kU/L lysophospholipase was added to each sample. Next, the reaction mix was incubated at 37°C for 5 min, and the absorbance was measured at 570/700 nm (test/reference wavelength).

Assays

Plasma concentrations of tumor necrosis factor (TNF)-α and interleukin (IL)-1β were determined using a mouse TNF-α ELISA and mouse IL-1β ELISA kit (Excell, Shanghai, China). Plasma level of lysophosphatidic acid (LPA) was analyzed using the LPA Assay kit (Echelon Biosciences, Salt Lake City, UT).

Statistical Analysis

Data are reported as mean ± SEM. For GTT/ITT studies with multiple time points, we performed two-way repeated-measures ANOVA to test differences in means between SR-A$^{+/+}$ and SR-A$^{-/-}$ groups. When ANOVA was significant, t tests were applied. Analysis for areas under the GTT and ITT curves was performed using GraphPad Prism 5 software. For comparison of data between two groups at a single time point, unpaired t tests were performed.

RESULTS

Loss of SR-A Leads to a Deterioration in Insulin Sensitivity in *ob/ob* Mice

To assess the role of SR-A in obesity-induced insulin resistance, we generated SR-A$^{-/-}$ mice with a

leptin-deficient background (SR-A$^{-/-}$*ob/ob*). We found that SR-A$^{-/-}$*ob/ob* mice gained more body weight (Fig. 1A) and epididymal fat pad weight (Fig. 1B). Meanwhile, SR-A$^{-/-}$*ob/ob* mice displayed higher levels of fasting blood glucose (~24%) (Fig. 1C) and insulin (~53%) (Fig. 1D). Morphometric analysis revealed that adipocyte size of SR-A$^{-/-}$*ob/ob* mice was similar to that of SR-A$^{+/+}$*ob/ob* mice (Fig. 1E).

The insulin response of SR-A$^{-/-}$*ob/ob* mice was significantly lower than in SR-A$^{+/+}$*ob/ob* mice as assayed by the GTT (Fig. 1F), indicating an overall deterioration in insulin action as a result of SR-A deletion. We next performed an ITT and found that lack of SR-A led to a decrease in systemic insulin sensitivity (Fig. 1G). These in vivo findings are corroborated by the measures of insulin signaling in isolated adipose tissue, in which insulin-stimulated insulin receptor (IR) (Fig. 1H) and Akt phosphorylation (Fig. 1I) were decreased in the SR-A$^{-/-}$*ob/ob* mice.

Loss of SR-A Promotes a Skewed M1/M2 ATM Polarization in *ob/ob* Mice

Inflammation is an important pathological process that links obesity and insulin resistance. To explore how SR-A impacts insulin sensitivity, we hypothesized that SR-A deficiency would result in stronger inflammatory response by influencing macrophage recruitment or by shifting macrophage polarization within the adipose tissue. To test this hypothesis, we first measured the expression levels of macrophage/myeloid cell–specific genes (*Cd68*, *Emr1*, *Cd11b*, and *Csf1r*) in mouse epididymal fat tissue. Surprisingly, there was no difference between SR-A$^{-/-}$*ob/ob* and SR-A$^{+/+}$*ob/ob* mice in expression levels of these genes (except for *Emr1*) (Fig. 2A). We performed immunohistochemical staining and enumerated the number of F4/80-positive crown-like structures (CLSs) present in adipose tissue cross-sections. There was no significant difference in the numbers of CLSs and macrophages between SR-A$^{-/-}$*ob/ob* and SR-A$^{+/+}$*ob/ob* mice (Fig. 2D).

Next, we analyzed the phenotype of ATMs by measuring the expression of prototypical target genes in the isolated SVF where the macrophage population resides in epididymal fat pads (17). As shown in Fig. 2B, expression levels of characteristic M2 marker genes (*Arg1*, *Ym1*, *Mgl1*, and *Mrc2*) were decreased by 49.6–81.1% in SVF cells from SR-A$^{-/-}$*ob/ob* mice. Conversely, SR-A$^{-/-}$*ob/ob* SVF cells exhibited an enhancement (~1.1- to 2.7-fold) in the expression of M1 genes such as *Cd16*, *Cd32*, *Nos2*,

and SR-A$^{-/-}$*ob/ob* mice. The lysates were immunoblotted with Mrc2 and GAPDH antibody, and relative band intensities were normalized to GAPDH. $n = 3$. *H*: Flow cytometric analysis of the surface expression of F4/80 and CD11c in SVF cells. Isotype control Rat IgG1 Negative Control-488 was used to differentiate F4/80 positive/negative cells. Isotype control Rat IgG1 Negative Control-647 was used to differentiate CD11c and CD301 positive/negative cells (Supplementary Fig. 11). Representative plots of the F4/80$^+$CD11c$^+$ and F4/80$^+$CD11c$^-$ cell fractions. $n = 5$. *I*: Flow cytometric analysis of the surface expression of F4/80 and CD301 in SVF cells isolated from epididymal fat pads. Representative dot plots of the F4/80$^+$CD301$^+$ and F4/80$^+$CD301$^-$ cell fractions are shown. $n = 4$. Data are expressed as mean ± SEM. *$P < 0.05$; **$P < 0.01$; ***$P < 0.001$. FITC, fluorescein isothiocyanate. HP field, high-power field.
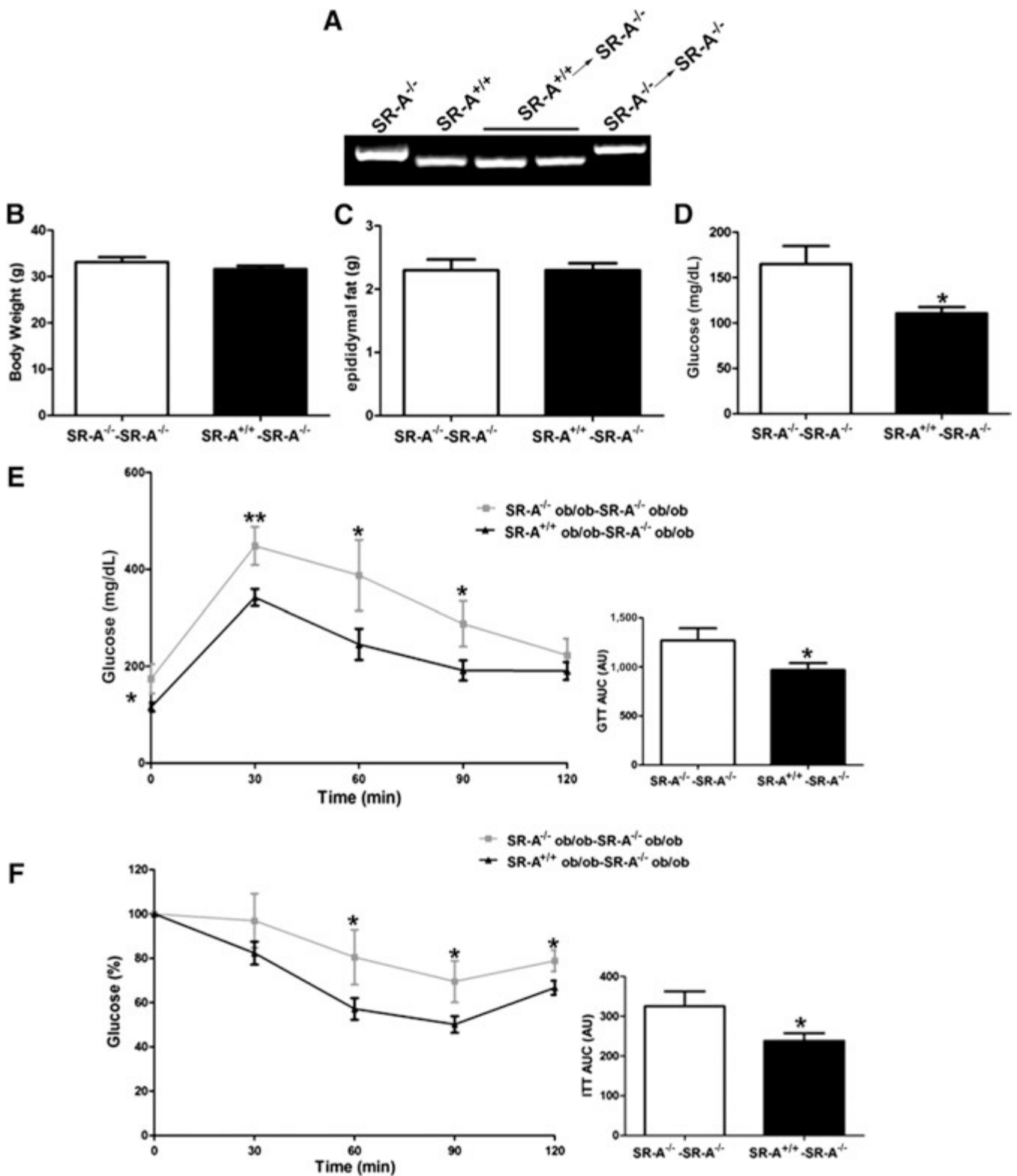
Figure 3—Transplantation of SR-A–expressing bone marrow rescues insulin sensitivity in SR-A$^{-/-}$ob/ob mice. A: PCR products showing the genotype of the SR-A locus in genomic DNA isolated from circulating white blood cells of SR-A$^{-/-}$ob/ob mice transplanted with SR-A$^{+/+}$ob/ob and SR-A$^{-/-}$ob/ob mice bone marrow. B–D: The SR-A$^{-/-}$ob/ob mice transplanted with SR-A$^{+/+}$ob/ob or SR-A$^{-/-}$ob/ob bone marrow were analyzed. The body weight (B), epididymal fat pad weight (C), and fasting plasma glucose levels (D) were measured. n = 6. E and F: GTT (E) and ITT (F) were performed. Area under the curve (AUC) of GTT and ITT was calculated and is expressed as arbitrary units (AU). n = 6. Data are expressed as mean ± SEM. *P < 0.05; **P < 0.01.
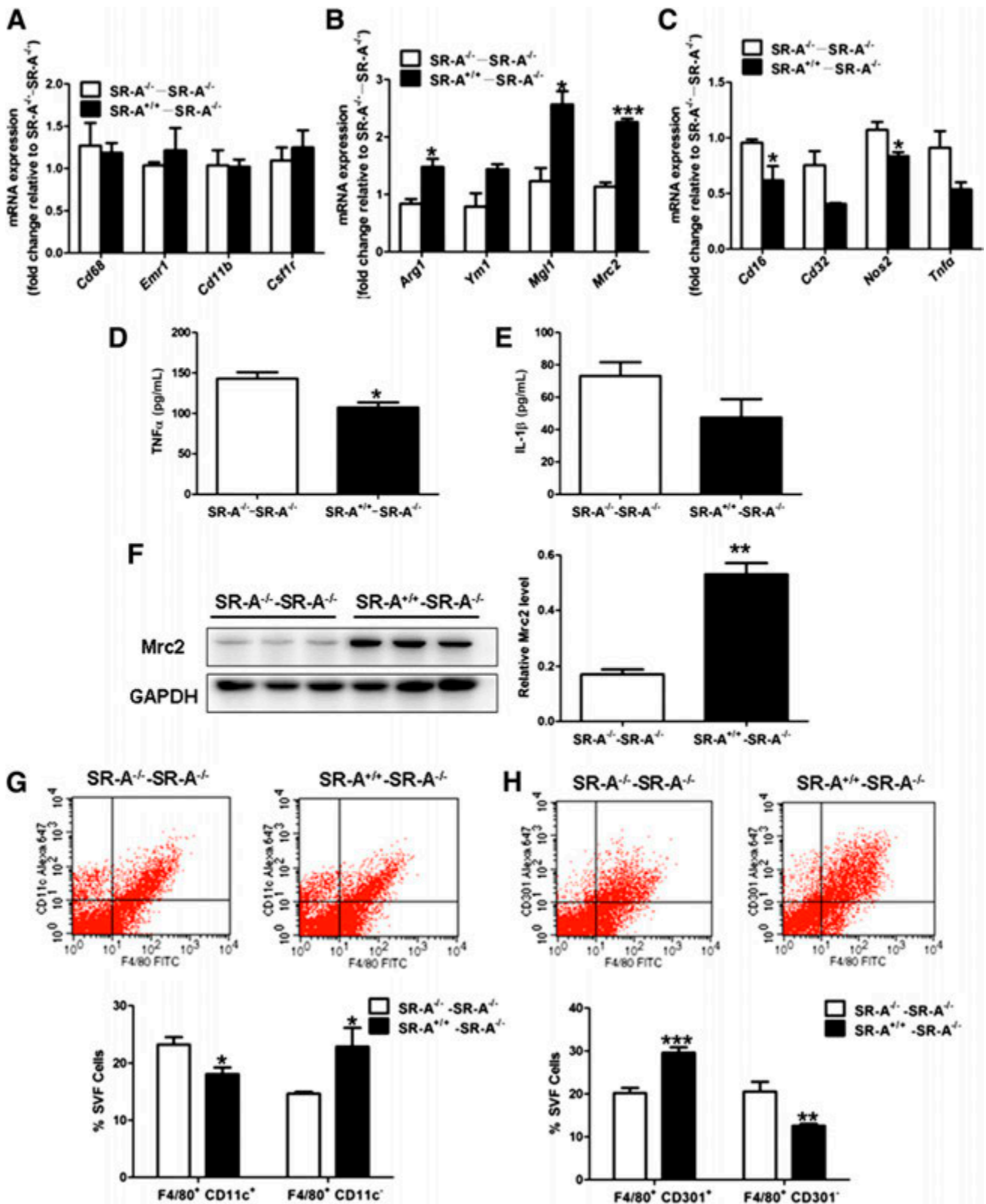
Figure 4—SR-A modulates macrophage polarization in adipose tissue. *A*: Expression of macrophage/myeloid cell–specific genes was analyzed in epididymal fat tissue. Expression levels were normalized first to those of GAPDH and then further normalized to the levels of SR-A$^{-/-}$ob/ob–SR-A$^{-/-}$ob/ob cells. n = 5. *B* and *C*: SVF cells were isolated from epididymal fat pads. Levels of mRNA expression of M2 macrophage–associated genes (*B*) and M1 macrophage–associated genes (*C*) were analyzed. Expression levels were normalized first to those of GAPDH and then further normalized to the levels of SR-A$^{-/-}$ob/ob–SR-A$^{-/-}$ob/ob cells. n = 5. *D* and *E*: Plasma levels of TNF-α (*D*) and IL-1β (*E*) were measured using ELISA assay. n = 6. *F*: The blots of Mrc2 in adipose tissue. The lysates were immunoblotted with Mrc2 and GAPDH antibody, and relative band intensities were normalized to GAPDH. n = 3. *G*: Flow cytometric analysis of the surface

and *Tnfα* (Fig. 2*C*), suggesting that SR-A deficiency resulted in a pivoted ATM differentiation toward the M1 phenotype. We also found that the circulating levels of TNF-α and IL-1β were also increased in SR-A$^{-/-}$*ob/ob* mice (Fig. 2*E* and *F*), and the protein level of Mrc2 was decreased in SR-A$^{-/-}$*ob/ob* mice (Fig. 2*G*).

The M1/M2 ATM subpopulations were also analyzed by flow cytometry. CD11c is a marker to distinguish M1 and M2 macrophages. The CD11c$^+$ macrophages (M1 subtype) account for the majority of increased ATMs in obesity and overexpress proinflammatory cytokines compared with the CD11c$^-$ ATMs (M2 subtype) (18). On the contrary, CD301-positive F4/80 macrophages are believed to exclusively an M2 fraction (19). We found that the percentage of F4/80$^+$CD11c$^-$ cells was decreased in the SR-A$^{-/-}$*ob/ob* SVF cells compared with SR-A$^{+/+}$*ob/ob* SVF cells (20.1 ± 0.7% vs. 27.5 ± 1.8%) (Fig. 2*H*). Coincidently, the percentage of F4/80$^+$CD301$^+$ cells in SR-A$^{-/-}$*ob/ob* SVF cells was lower than those in SR-A$^{+/+}$*ob/ob* cells (38.8 ± 2.1% vs. 46.4 ± 1.6%) (Fig. 2*I*).

Transplantation of SR-A Expressing Bone Marrow Rescues Insulin Sensitivity in SR-A$^{-/-}$ *ob/ob* Mice

To further identify a causal link between SR-A and obesity-induced insulin resistance, we performed bone marrow transplantation to generate chimeric SR-A$^{-/-}$*ob/ob* mice carrying bone marrow from either SR-A$^{+/+}$*ob/ob* or SR-A$^{-/-}$*ob/ob* mice. Examination of genomic DNA, isolated from circulating white blood cells, indicated that the transplanted animals were highly chimeric, as evidenced by the genotype observed in the SR-A allele (Fig. 3*A*). Measurements of body weight and epididymal fat pad weight showed no significant differences between SR-A$^{-/-}$*ob/ob* mice carrying SR-A$^{+/+}$*ob/ob* bone marrow and carrying SR-A$^{-/-}$*ob/ob* bone marrow (Fig. 3*B* and *C*). However, SR-A$^{-/-}$*ob/ob* mice transplanted by SR-A$^{+/+}$*ob/ob* bone marrow displayed reduced fasting blood glucose (~49%) (Fig. 3*D*). Upon assessment of GTT and ITT, the first impression was that insulin sensitivity in SR-A$^{-/-}$*ob/ob* mice was improved by transplantation with SR-A$^{+/+}$*ob/ob* bone marrow (Fig. 3*E* and *F*), suggesting that the beneficial effect of SR-A on obesity-induced insulin resistance could be derived from its activity bound to macrophages.

We then measured the expression levels of macrophage/myeloid cell–specific genes (*Cd68*, *Emr1*, *Cd11b*, and *Csf1r*) in epididymal fat tissues. No obvious difference was found between the SR-A$^{-/-}$*ob/ob* mice transplanted with the SR-A$^{+/+}$*ob/ob* bone marrow and transplanted with the SR-A$^{-/-}$*ob/ob* bone marrow (Fig. 4*A*).

However, expression levels of M2 (*Arg1*, *Ym1*, *Mgl1*, and *Mrc2*) genes in epididymal fat pads were increased (~1.8- to 2.1-fold) and those of M1 genes (*Cd16*, *Cd32*, *Nos2*, and *Tnfα*) were decreased by 22.1–46.4% in the SR-A$^{+/+}$*ob/ob* bone marrow–transplanted mice compared with the SR-A$^{-/-}$*ob/ob* bone marrow–transplanted mice (Fig. 4*B* and *C*). The circulating level of TNF-α, but not IL-1β, was significantly reduced (Fig. 4*D* and *E*) and Mrc2 level was significantly increased after SR-A$^{+/+}$*ob/ob* bone marrow was transplanted into SR-A$^{-/-}$*ob/ob* mice (Fig. 4*F*). Consistently, flow cytometry analysis showed that the F4/80$^+$CD11c$^-$ population in the SVF cells was dramatically increased in the SR-A$^{-/-}$*ob/ob* mice transplanted with SR-A$^{+/+}$ *ob/ob* bone marrow compared with those transplanted with SR-A$^{-/-}$*ob/ob* bone marrow (22.9 ± 3.3% vs. 14.6 ± 0.3%) (Fig. 4*G*). Similarly, the F4/80$^+$CD301$^+$ double-positive cells in the SVF cells were also dramatically increased (29.6 ± 1.3% vs. 20.2 ± 1.2%) (Fig. 4*H*).

Loss of SR-A Aggravates Insulin Resistance in DIO Mice

As a genetic model for the study on obesity and insulin resistance, *ob/ob* mice have certain limitations in part because these animals suffer from immune deficiencies, reproductive hormone abnormalities, and changes in bone homeostasis that may complicate the analysis of inflammation in adipose tissue (20,21). Mice fed by a high-fat and high-carbohydrate diet can develop DIO, which is believed to more faithfully mirror human obesity. Thus, we also used HFD to feed SR-A$^{-/-}$ mice for 16 weeks to determine the impact of SR-A on obesity-induced insulin resistance.

As expected, body weight gain in HFD-fed mice significantly outpaced chow diet–fed mice, but there was no significant difference in body weight (Fig. 5*A*) and epididymal fat pad weight (Fig. 5*B*) between SR-A$^{+/+}$ and SR-A$^{-/-}$ mice fed by either diet. There also was no detectable difference in food intake (data not shown). Nevertheless, SR-A$^{-/-}$ mice with DIO had higher fasting levels of glucose (~15%) (Fig. 5*C*) and insulin (~33%) (Fig. 5*D*). Morphometric analysis revealed that adipocyte size of SR-A$^{-/-}$ mice was similar to that of SR-A$^{+/+}$ mice (Fig. 5*E*). Glucose levels in a fasted state as well as during GTT and ITT were significantly increased in SR-A$^{-/-}$ mice (Fig. 5*F* and *G*). Meanwhile, insulin-stimulated IR and Akt phosphorylation under HFD conditions were decreased in SR-A$^{-/-}$ adipose tissue (Fig. 5*H* and *I*). CD36 is a class B scavenger receptor that also impacts insulin sensitivity (22–24). Western blot analysis showed

expression of F4/80 and CD11c from SVF cells isolated from epididymal fat pad. Representative plots of the F4/80$^+$CD11c$^+$ and F4/80$^+$CD11c$^-$ cell fractions are shown. *n* = 4. *H*: Flow cytometric analysis of the surface expression of F4/80 and CD301 from the SVF cells isolated from epididymal fat pads. Representative plots of the F4/80$^+$CD301$^+$ and F4/80$^+$CD301$^-$ cell fractions are shown. *n* = 4. Data are expressed as mean ± SEM. *P < 0.05; **P < 0.01; ***P < 0.001. FITC, fluorescein isothiocyanate.
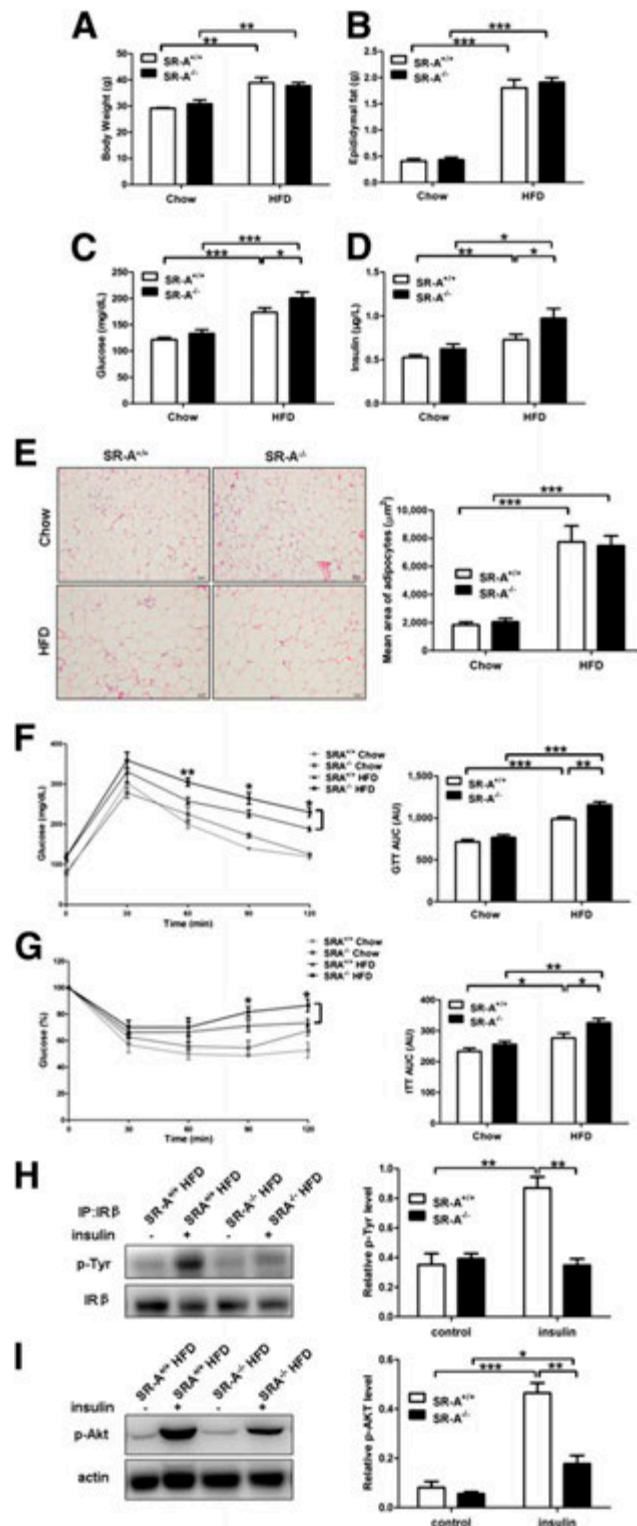
Figure 5—Loss of SR-A on GTT and ITT in HFD-fed mice. A–E: The SR-A$^{+/+}$ and SR-A$^{-/-}$ mice fed with a chow diet or HFD for 16 weeks were analyzed. The body weight (A), epididymal fat pad weight (B), fasting plasma glucose (C), and fasting serum insulin concentrations (D) were measured. Histological sections of epididymal fat pads were quantitatively analyzed by Image-Pro Plus software in adipocyte size (E). n = 6. F and G: GTT (F) and ITT (G) were performed in SR-A$^{+/+}$ and SR-A$^{-/-}$ mice fed with either HFD or chow diet after 16 weeks. Areas under the curve (AUC) of GTT and ITT were calculated and are expressed as arbitrary units (AU). n = 6. H and I: The representative blots of insulin signaling in the adipose tissue of mice fed with an HFD and administered with insulin. The lysates were immunoprecipitated with IRβ antibody and immunoblotted with phospho-Tyr (p-Tyr) and IRβ antibody. Relative band intensities were normalized to IRβ. n = 3 (H). The lysates were immunoblotted with p-Akt and β-actin antibody, and relative band intensities were normalized to β-actin. n = 3 (I). Data are expressed as mean ± SEM. *P < 0.05; **P < 0.01; ***P < 0.001. IP, immunoprecipitation.
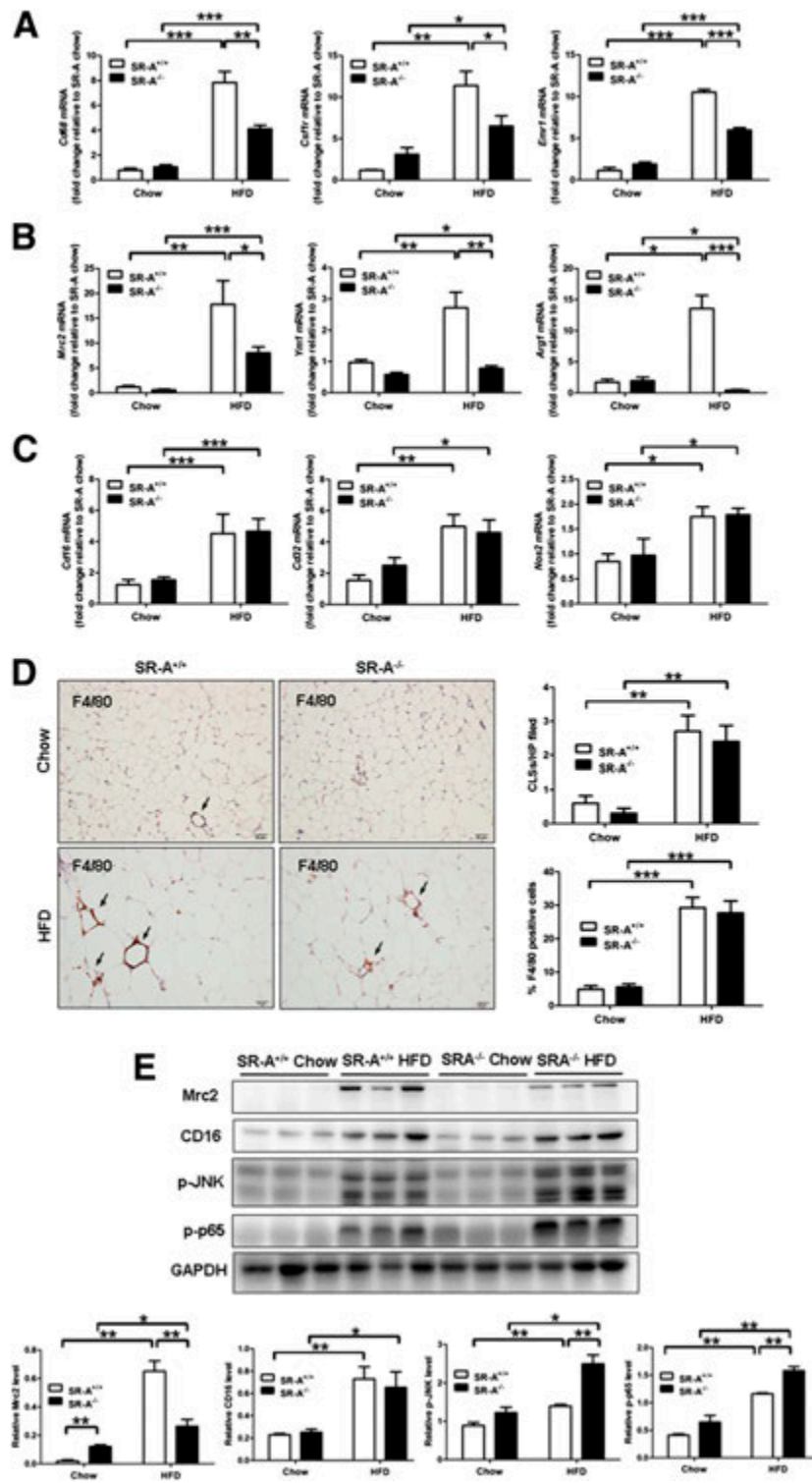
Figure 6—Loss of SR-A on recruitment of macrophages into adipose tissue and immunogenic phenotype of isolated ATMs. A: Expression of macrophage/myeloid cell–specific genes was analyzed in epididymal fat tissue. Expression levels were normalized first to those of GAPDH and then further normalized to the levels of SR-A$^{+/+}$ chow mice. $n = 5$. B and C: Epididymal fat tissues were isolated from the SR-A$^{+/+}$ and SR-A$^{-/-}$ mice fed with a chow diet or HFD for 16 weeks. Levels of mRNA expression of M2 macrophage–associated genes (B) and M1 macrophage–associated genes (C) were analyzed. Expression levels were normalized first to those of GAPDH and then further normalized to the levels of SR-A$^{+/+}$ mice with a chow diet. $n = 5$. D: Immunohistochemical staining for F4/80 in epididymal fat pad sections. The number of CLSs (brown staining [see arrows]) and F4/80-positive cells relative to total number of cells was determined (6–10 images at ×20 magnification were analyzed per mouse). $n = 5$. E: The blots of Mrc2, CD16, phospho (p)–Jun NH$_2$-terminal kinase (p-JNK), p-p65, and GAPDH in the adipose tissue of SR-A$^{+/+}$ and SR-A$^{-/-}$ mice. Relative band intensities were normalized to GAPDH. $n = 3$. Data are expressed as mean ± SEM. *$P < 0.05$; **$P < 0.01$; ***$P < 0.001$. HP field, high-power field.

that no significant difference in CD36 expression in ATMs was found between SR-A$^{+/+}$ and SR-A$^{-/-}$ mice (Supplementary Fig. 1).

Loss of SR-A Markedly Inhibits Infiltration of M2 Macrophages in HFD-Fed Mouse Adipose Tissue

To clarify whether SR-A could modulate macrophage polarization in DIO conditions, we examined the infiltrated macrophage content and phenotype in the mouse epididymal adipose tissue. HFD feeding caused a progressive increase in the expression levels of macrophage-specific markers (*Cd68*, *Csf1r*, and *Emr1*). However, they were decreased by 42.9–47.4% in the SR-A$^{-/-}$ adipose tissue (Fig. 6*A*). The relative levels of M2 marker genes (*Mrc2, Ym1,* and *Arg1*) were decreased by 54.9–96.9% in the adipose tissue of SR-A$^{-/-}$ mice (Fig. 6*B*), but the expression levels of M1 genes (*Cd16, Cd32,* and *Nos2*) were not significantly affected by SR-A deficiency in HFD-fed mice (Fig. 6*C*). There was no significant difference in the numbers of CLSs and macrophages between SR-A$^{-/-}$ and SR-A$^{+/+}$ mice (Fig. 6*D*).

The circulating level of IL-1β (Supplementary Fig. 2) and of Mrc2 (Fig. 6*E*) was dramatically increased in HFD-fed SR-A$^{-/-}$ mice. SR-A deficiency also caused activation of inflammatory signaling (Jun NH$_2$-terminal kinase [JNK] and nuclear factor-κB) in adipose tissue in HFD-fed mice (Fig. 6*E*). In accordance with the gene expression, flow cytometry analysis showed a similar macrophage phenotype in the adipose tissue (Supplementary Fig. 3). Together, we conclude that SR-A may preferentially regulate M2 macrophage infiltration or differentiation in DIO mice. Furthermore, we also found an increased M1 accumulation (F4/80$^+$CD11c$^+$ cells) in HFD-fed mice compared with chow-fed conditions either in SR-A$^{+/+}$ or SR-A$^{-/-}$ mice (Supplementary Fig. 4).

SR-A Is Required for a Deflected M2/M1 Macrophage Polarization

To further identify the definite role of SR-A in macrophage polarization, we used LPS or IL-4, well-established M1 or M2 polarizing agents (25), to treat cultured mouse PM in vitro. It has been shown that SR-A is upregulated by treatment with IL-4 but downregulated after LPS treatment as reported (data not shown) (26–28). We examined the effect of SR-A deficiency on macrophage polarization in vitro. As shown in Fig. 7*A*, administration of IL-4 caused a dramatic increase in mRNA levels of characteristic M2 marker genes (*Arg1, Ym1,* and *Mgl1*) in SR-A$^{+/+}$ PMs. This was significantly attenuated by 50.9–94.2% in SR-A$^{-/-}$ PMs, indicating that SR-A is a likely prerequisite for M2 activation. By contrast, SR-A deficient macrophages exhibited an enhancement in mRNA levels of M1 genes (*Cd32, Tnfα,* and *Nos2* [~1.5- to 2.0-fold]) after LPS stimulation (Fig. 7*B*). Similar changes were found in the production of TNF-α and IL-1β by macrophages (Fig. 7*C* and *D*).

It is known that GM-CSF induces bone marrow cell–derived macrophages to differentiate toward M1 subtype

and that M-CSF induces M2 differentiation (14). We found that SR-A deficiency caused a dramatic loss in M2 differentiation-stimulating ability by M-CSF in bone marrow–derived macrophages as measurements of mRNA levels of *Arg1*, *Ym1*, and *Mgl1* genes (Supplementary Fig. 5*A*). In accordance with this, M1 polarization induced by GM-CSF was increased in SR-A$^{-/-}$ macrophages compared with SR-A$^{+/+}$ cells (Supplementary Fig. 5*B*). SR-A deficiency impaired macrophage phagocytosis activity, a major function of SR-A (Supplementary Fig. 6*A*), but did not obviously affect macrophage chemotaxist function (Supplementary Fig. 6*B*).

To further determine the mechanism underlying SR-A–dependent M2 activation, we examined the activation of STAT6, a well-known molecule in M2 macrophage polarization (29). As expected, the increased STAT6 phosphorylation after IL-4 treatment was abolished in SR-A$^{-/-}$ PMs (Fig. 7*E*), suggesting that STAT6 is involved in SR-A mediated M2 macrophage polarization.

LPC Activates SR-A–Mediated M2 Macrophage Polarization

To fully understand the modulating effect of SR-A on macrophage polarization in obesity, we asked how SR-A could be activated in obesity-induced insulin resistance. LPC is an endogenous ligand for SR-A with diverse functions in obesity and insulin resistance (30,31). We found that LPC levels in plasma, adipose tissue, and adipocytes, but not in adipocyte membrane fractions, were significantly elevated in SR-A$^{-/-}$*ob/ob* mice compared with SR-A$^{+/+}$*ob/ob* mice (Fig. 8*A*–*D*). Similar results were also obtained in the DIO mouse model (Supplementary Fig. 7). We also measured levels of other lipids including LPA, free fatty acid (FFA), triglycerides (TG), and total cholesterol in plasma and TG in adipose tissue. No significant difference in levels of these lipids, except for FFA, was found between SR-A$^{+/+}$ and SR-A$^{-/-}$ mice (Supplementary Fig. 8). Elevated plasma level of FFA in obesity is normally caused by increased release of FFA from the enlarged adipose tissue mass. Thus, these results suggest an association between LPC and SR-A in the states of obesity-induced insulin resistance.

To verify whether LPC is a functionally relevant SR-A ligand, we further examined the effect of LPC on SR-A–mediated macrophage polarization in vitro. As shown in Fig. 8*E*, administration of LPC caused an increase in expression levels of typical M2 marker genes (*Arg1, Ym1,* and *Mgl1*) in SR-A$^{+/+}$ PMs. This effect was abolished by SR-A deletion, indicating the requirement of SR-A for LPC-induced M2 macrophage polarization. Meanwhile, LPC was shown to exert a mild suppressive effect on M1 polarization (Fig. 8*F*). Similar results were obtained in bone marrow cells (Supplementary Fig. 9). To indicate the specificity of LPC, we also tested the effect of LPA and lysophosphatidylethenolamine on macrophage polarization. RT-PCR analysis showed that macrophage polarization was not influenced by treatment with these
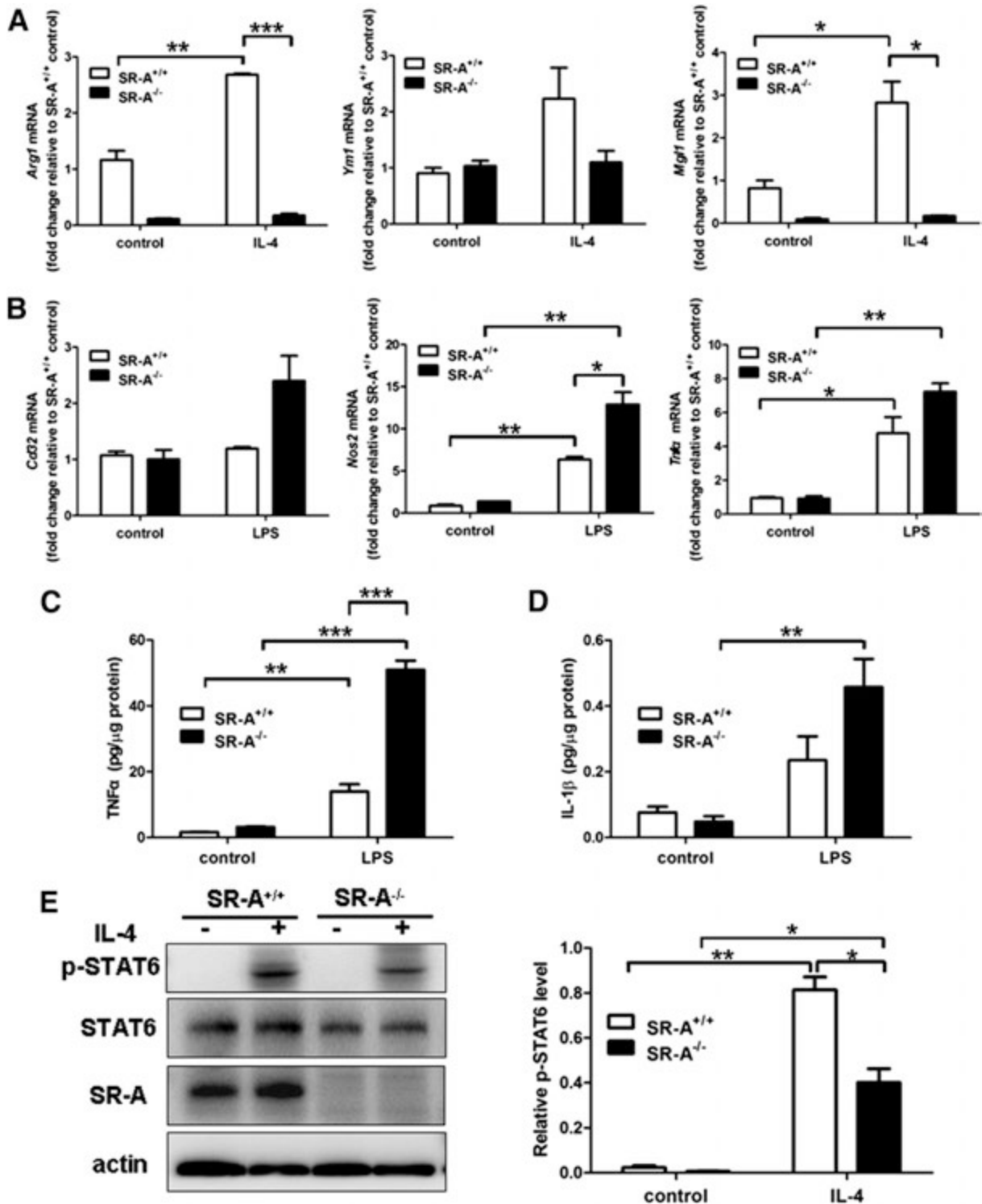
Figure 7—SR-A is requisite for IL-4–induced M2 macrophage polarization. *A*: mRNA levels of M2 macrophage–associated genes in mice PMs. PMs were harvested and cultured in vitro. After 1 day, PMs were treated with mouse IL-4 (5 ng/mL) for 16 h. Expression levels of mRNA were normalized first to those of GAPDH and then further normalized to the levels of SR-A$^{+/+}$ control PMs. $n = 4$. *B*: mRNA levels of M1 macrophage–associated genes in mice PMs. PMs were harvested and cultured in vitro. After 1 day, PMs were treated with mouse LPS (100 ng/mL) for 16 h. Levels of mRNA were normalized first to those of GAPDH and then further normalized to the levels of SR-A$^{+/+}$ control PMs. $n = 4$. *C* and *D*: TNF-α (*C*) and IL-1β (*D*) levels were measured using ELISA assay. PMs were harvested and cultured in vitro. After 1 day, PMs were treated with mouse LPS (100 ng/mL) for 16 h. $n = 4$. *E*: Mouse PMs were treated with IL-4 (5 ng/mL) for 30 min. The lysates of each sample were subjected to immunoblotting with antibodies against p-STAT6, STAT6, SR-A, or β-actin as indicated. Representative blots are presented, and relative band intensities were normalized to STAT6. $n = 3$. Data are expressed as mean ± SEM. *$P < 0.05$; **$P < 0.01$; ***$P < 0.001$.
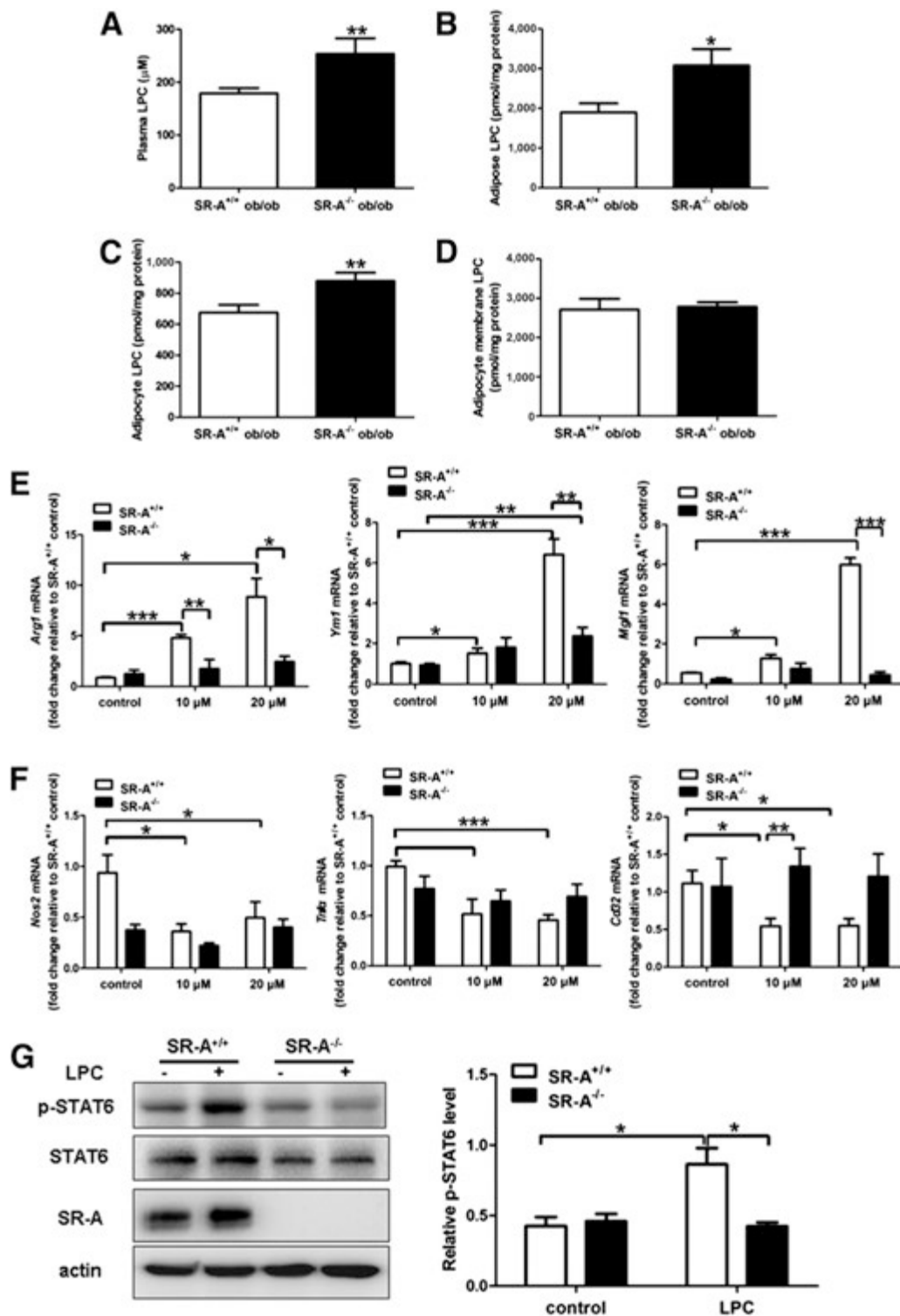
Figure 8—LPC is required for SR-A–mediated M2 macrophage polarization. LPC levels in plasma (*A*), in epididymal fat tissue (*B*), in adipocytes (*C*), and in adipocyte membrane fractions (*D*) were measured in 9-week-old SR-A$^{+/+}$ *ob/ob* and SR-A$^{-/-}$ *ob/ob* mice. $n = 4$–6. *E*: mRNA levels of M2 macrophage–associated genes in mice PMs. PMs were harvested and cultured in vitro. After 1 day, PMs were treated with LPC (10 or 20 μmol/L) for 16 h. Expression levels of mRNA were normalized first to those of GAPDH and then further normalized to the levels of SR-A$^{+/+}$ control PMs. $n = 4$. *F*: mRNA levels of M1 macrophage–associated genes in mice PMs. PMs were harvested and cultured in vitro. After 1 day, PMs were treated with mouse LPC (10 or 20 μmol/L) for 16 h. Levels of mRNA expression were normalized first to those of GAPDH and then further normalized to the levels of SR-A$^{+/+}$ control PMs. $n = 4$. *G*: Mouse PMs were treated with LPC (20 μmol/L) for 30 min. The lysates of each sample were subjected to immunoblotting with antibodies against p-STAT6, STAT6, SR-A, or β-actin as indicated. Representative blots are presented, and relative band intensities were normalized to STAT6. $n = 3$. Data are expressed as mean ± SEM. *$P < 0.05$; **$P < 0.01$; ***$P < 0.001$.

two substances (Supplementary Fig. 10). Finally, we showed that the increased STAT6 phosphorylation after LPC treatment was abolished in SR-A$^{-/-}$ PMs (Fig. 8G), suggesting that STAT6 might be involved in LPC/SR-A–mediated M2 macrophage polarization.

DISCUSSION

Chronic inflammation is a central contributing factor in the development of obesity-induced insulin resistance. It is known that PRRs play a key role by recognizing a variety of endogenous molecules derived from tissue injuries and eliciting sterile inflammation (32,33). Emerging evidence highlights that, as a key constituent of the PRR superfamily, SR-A is involved in a range of disease models by immune modulation. For instance, SR-A exerts a protective effect against ischemic myocardium injury via the modification of inflammatory cytokines (34,35). To date, the role of SR-A in insulin resistance remains largely ill defined. We show here that knockout of SR-A could deteriorate obesity-induced insulin resistance in mouse adipose tissue.

SR-A is expressed primarily in macrophages. Macrophages can acquire distinct functional phenotypes in the microenvironment that they dwell in or migrate to. We reveal that deletion of SR-A leads to an M1-favoring polarization for ATMs in obese mice. Of note, SR-A levels seem to fluctuate in macrophages during stimuli-induced polarization, indicative of a potential role for SR-A in this process. We found that the moderately increased response of SR-A$^{-/-}$ PMs to LPS in vitro and SR-A was upregulated in M2 macrophage differentiation. Based on these observations, we postulate that SR-A may modulate macrophage differentiation toward M2 subtype in the adipose tissue. This notion is supported by the results that SR-A deficiency dramatically impairs the ability of IL-4 and M-CSF to activate M2 polarization. However, a more important question is how SR-A–mediated M2 polarization could be achieved, specifically in an obesity-skewed microenvironment, to alleviate obesity-induced insulin resistance. We report here that LPC, serving as an SR-A ligand, may feed to and steer SR-A to modulate macrophage polarization.

LPC, a highly abundant bioactive lysoglycerophospholipid in the circulation, is involved in regulating cellular proliferation and inflammation (36–38). Sakai et al. (30) have demonstrated that LPC is recognized by SR-A and required for the induction of macrophage growth. Consistent with our study, recent studies demonstrate that plasma LPC levels are reduced in mouse models of DIO and steatohepatitis (31,39). This seems to be causally linked to an observation that upregulation of SR-A in the adipose tissue is strongly associated with insulin resistance in nondiabetic humans (13). Our results clearly show that SR-A ablation results in increased LPC levels in plasma and adipose tissue in obese mice. Thus, a plausible explanation accounting for decreased LPC levels in obesity is that upregulation of SR-A

in ATMs in vivo can effectively clear off LPC from the circulation. Moreover, we demonstrate that the LPC-induced activation of the STAT6 pathway is abolished by SR-A deletion in macrophages. As a well-known transcription factor in regulating expression of M2 signatures *Arg1*, *Mrc1*, and *Ym1* (40,41), STAT6 may constitute the final node of the LPC/SR-A pathway to mediate macrophage differentiation toward M2 subtype.

In the current study, we have harnessed a genetic obese model (SR-A$^{-/-}$*ob/ob* mice) as well as a DIO model to conduct detailed experiments of macrophage biology, obesity, and insulin resistance. Our in vivo findings demonstrate that lack of SR-A aggravates obesity-induced insulin resistance in both models. The weight gain of SR-A$^{-/-}$*ob/ob* mice is more pronounced than in SR-A$^{+/+}$*ob/ob* mice. Yet, this phenotype is not confirmed by the bone marrow transplantation model and is also not seen in mice fed with an HFD. Maybe SR-A by itself is not a dominant regulator in lipid metabolism (42,43). The global SR-A deficiency–induced weight change in *ob/ob* mice seems to be correctable by confining SR-A deficiency to hematopoietic cells. However, *ob/ob* mice are deficient for production of leptin, which results in obesity (44). The mechanism underlying deletion of SR-A aggravating leptin deficiency–induced obesity is worth further investigation.

In conclusion, we have clearly demonstrated that LPC/SR-A may inhibit obesity-induced insulin resistance by promoting M2 macrophage polarization. Combined with our previous findings that SR-A regulates the inflammatory response by programming M2 polarization in ischemic tissues (34,45), this new piece of information reinforces the notion that SR-A may serve as a novel "sensor" to environmental inputs such as LPC to shape macrophage identity and function in disease states.

References

1. Kahn SE, Hull RL, Utzschneider KM. Mechanisms linking obesity to insulin resistance and type 2 diabetes. Nature 2006;444:840–846

2. Lumeng CN, Saltiel AR. Inflammatory links between obesity and metabolic disease. J Clin Invest 2011;121:2111–2117

3. Saberi M, Woods NB, de Luca C, et al. Hematopoietic cell-specific deletion of toll-like receptor 4 ameliorates hepatic and adipose tissue insulin resistance in high-fat-fed mice. Cell Metab 2009;10:419–429

4. Chawla A, Nguyen KD, Goh YP. Macrophage-mediated inflammation in metabolic disease. Nat Rev Immunol 2011;11:738–749

5. Han MS, Jung DY, Morel C, et al. JNK expression by macrophages promotes obesity-induced insulin resistance and inflammation. Science 2013; 339:218–222

6. Oh DY, Morinaga H, Talukdar S, Bae EJ, Olefsky JM. Increased macrophage migration into adipose tissue in obese mice. Diabetes 2012;61: 346–354

7. Gordon S, Martinez FO. Alternative activation of macrophages: mechanism and functions. Immunity 2010;32:593–604

8. Odegaard JI, Ricardo-Gonzalez RR, Goforth MH, et al. Macrophage-specific PPARgamma controls alternative activation and improves insulin resistance. Nature 2007;447:1116–1120

9. Ben J, Gao S, Zhu X, et al. Glucose-regulated protein 78 inhibits scavenger receptor A-mediated internalization of acetylated low density lipoprotein. J Mol Cell Cardiol 2009;47:646–655

10. Krieger M, Herz J. Structures and functions of multiligand lipoprotein receptors: macrophage scavenger receptors and LDL receptor-related protein (LRP). Annu Rev Biochem 1994;63:601–637

11. Zhu XD, Zhuang Y, Ben JJ, et al. Caveolae-dependent endocytosis is required for class A macrophage scavenger receptor-mediated apoptosis in macrophages. J Biol Chem 2011;286:8231–8239

12. Ben J, Jin G, Zhang Y, et al. Class A scavenger receptor deficiency exacerbates lung tumorigenesis by cultivating a procarcinogenic microenvironment in humans and mice. Am J Respir Crit Care Med 2012;186: 763–772

13. Rasouli N, Yao-Borengasser A, Varma V, et al. Association of scavenger receptors in adipose tissue with insulin resistance in nondiabetic humans. Arterioscler Thromb Vasc Biol 2009;29:1328–1335

14. Satoh T, Takeuchi O, Vandenbon A, et al. The Jmjd3-Irf4 axis regulates M2 macrophage polarization and host responses against helminth infection. Nat Immunol 2010;11:936–944

15. Folch J, Lees M, Sloane Stanley GH. A simple method for the isolation and purification of total lipides from animal tissues. J Biol Chem 1957;226:497–509

16. Kishimoto T, Soda Y, Matsuyama Y, Mizuno K. An enzymatic assay for lysophosphatidylcholine concentration in human serum and plasma. Clin Biochem 2002;35:411–416

17. Oh DY, Talukdar S, Bae EJ, et al. GPR120 is an omega-3 fatty acid receptor mediating potent anti-inflammatory and insulin-sensitizing effects. Cell 2010;142:687–698

18. Li P, Fan W, Xu J, et al. Adipocyte NCoR knockout decreases PPARγ phosphorylation and enhances PPARγ activity and insulin sensitivity. Cell 2011;147:815–826

19. Atochina O, Da'dara AA, Walker M, Harn DA. The immunomodulatory glycan LNFPIII initiates alternative activation of murine macrophages in vivo. Immunology 2008;125:111–121

20. Swerdloff RS, Batt RA, Bray GA. Reproductive hormonal function in the genetically obese (ob/ob) mouse. Endocrinology 1976;98:1359–1364

21. Swerdloff RS, Peterson M, Vera A, Batt RA, Heber D, Bray GA. The hypothalamic-pituitary axis in genetically obese (ob/ob) mice: response to luteinizing hormone-releasing hormone. Endocrinology 1978;103:542–547

22. Liang CP, Han S, Okamoto H, et al. Increased CD36 protein as a response to defective insulin signaling in macrophages. J Clin Invest 2004;113:764–773

23. Kennedy DJ, Kuchibhotla S, Westfall KM, Silverstein RL, Morton RE, Febbraio MA. A CD36-dependent pathway enhances macrophage and adipose tissue inflammation and impairs insulin signalling. Cardiovasc Res 2011;89:604–613

24. Nicholls HT, Kowalski G, Kennedy DJ, et al. Hematopoietic cell-restricted deletion of CD36 reduces high-fat diet-induced macrophage infiltration and improves insulin signaling in adipose tissue. Diabetes 2011;60:1100–1110

25. Usher MG, Duan SZ, Ivaschenko CY, et al. Myeloid mineralocorticoid receptor controls macrophage polarization and cardiovascular hypertrophy and remodeling in mice. J Clin Invest 2010;120:3350–3364

26. Ganesan S, Faris AN, Comstock AT, Sonstein J, Curtis JL, Sajjan US. Elastase/LPS-exposed mice exhibit impaired innate immune responses to bacterial challenge: role of scavenger receptor A. Am J Pathol 2012;180: 61–72

27. Józefowski S, Arredouani M, Sulahian T, Kobzik L. Disparate regulation and function of the class A scavenger receptors SR-AI/II and MARCO. J Immunol 2005;175:8032–8041

28. Nikolic D, Calderon L, Du L, Post SR. SR-A ligand and M-CSF dynamically regulate SR-A expression and function in primary macrophages via p38 MAPK activation. BMC Immunol 2011;12:37

29. Lawrence T, Natoli G. Transcriptional regulation of macrophage polarization: enabling diversity with identity. Nat Rev Immunol 2011;11:750–761

30. Sakai M, Miyazaki A, Hakamata H, et al. The scavenger receptor serves as a route for internalization of lysophosphatidylcholine in oxidized low density lipoprotein-induced macrophage proliferation. J Biol Chem 1996;271: 27346–27352

31. Tanaka N, Matsubara T, Krausz KW, Patterson AD, Gonzalez FJ. Disruption of phospholipid and bile acid homeostasis in mice with nonalcoholic steatohepatitis. Hepatology 2012;56:118–129

32. Johnson GB, Brunn GJ, Platt JL. Activation of mammalian Toll-like receptors by endogenous agonists. Crit Rev Immunol 2003;23:15–44

33. Lee JY, Hwang DH. The modulation of inflammatory gene expression by lipids: mediation through Toll-like receptors. Mol Cells 2006;21:174–185

34. Hu Y, Zhang H, Lu Y, et al. Class A scavenger receptor attenuates myocardial infarction-induced cardiomyocyte necrosis through suppressing M1 macrophage subset polarization. Basic Res Cardiol 2011;106:1311–1328

35. Tsujita K, Kaikita K, Hayasaki T, et al. Targeted deletion of class A macrophage scavenger receptor increases the risk of cardiac rupture after experimental myocardial infarction. Circulation 2007;115:1904–1911

36. Wang L, Radu CG, Yang LV, Bentolila LA, Riedinger M, Witte ON. Lysophosphatidylcholine-induced surface redistribution regulates signaling of the murine G protein-coupled receptor G2A. Mol Biol Cell 2005;16: 2234–2247

37. Xing F, Liu J, Mo Y, et al. Lysophosphatidylcholine up-regulates human endothelial nitric oxide synthase gene transactivity by c-Jun N-terminal kinase signalling pathway. J Cell Mol Med 2009;13:1136–1148

38. Sevastou I, Kaffe E, Mouratis MA, Aidinis V. Lysoglycerophospholipids in chronic inflammatory disorders: The PLA(2)/LPC and ATX/LPA axes. Biochim Biophys Acta 2013;1831:42–60

39. Barber MN, Risis S, Yang C, et al. Plasma lysophosphatidylcholine levels are reduced in obesity and type 2 diabetes. PLoS ONE 2012;7:e41456

40. Biswas SK, Mantovani A. Orchestration of metabolism by macrophages. Cell Metab 2012;15:432–437

41. Sica A, Bronte V. Altered macrophage differentiation and immune dysfunction in tumor development. J Clin Invest 2007;117:1155–1166

42. Moore KJ, Freeman MW. Scavenger receptors in atherosclerosis: beyond lipid uptake. Arterioscler Thromb Vasc Biol 2006;26:1702–1711

43. Moore KJ, Kunjathoor VV, Koehn SL, et al. Loss of receptor-mediated lipid uptake via scavenger receptor A or CD36 pathways does not ameliorate atherosclerosis in hyperlipidemic mice. J Clin Invest 2005;115:2192–2201

44. Alpers CE, Hudkins KL. Mouse models of diabetic nephropathy. Curr Opin Nephrol Hypertens 2011;20:278–284

45. Xu Y, Qian L, Zong G, et al. Class A scavenger receptor promotes cerebral ischemic injury by pivoting microglia/macrophage polarization. Neuroscience 2012;218:35–48